Gallium nitride: a versatile compound semiconductor as novel piezoelectric film for acoustic tweezer in manipulation of cancer cells

Chao Sun, Fangda Wu, David J. Wallis, Ming Hong Shen, Fan Yuan, Jian Yang, Jianzhong Wu, Zhihua Xie, Dongfang Liang, Hanlin Wang, Rowan Tickle, Roman Mikhaylov, Aled Clayton, You Zhou, Zhenlin Wu, Yongqing Fu, Wenpeng Xun, Xin Yang

***Abstract*—Gallium nitride (GaN) is a compound semiconductor which has advantages to generate new functionalities and applications due to its piezoelectric, pyroelectric, and piezo-resistive properties. Recently, surface acoustic wave (SAW) based acoustic tweezers were developed as an efficient and versatile tool to manipulate nano- and micro-particles aiming for patterning, separating and mixing biological and chemical components. Conventional piezoelectric materials to fabricate SAW devices such as lithium niobate suffers from its low thermal conductivity and incapability of fabricating multiphysical and integrated devices. This work piloted the development of a GaN-based Acoustic Tweezer (GaNAT) and its application in manipulating micro-particles and biological cells. For the first time, the GaN SAW device was integrated with a microfluidic channel to form an acoustofluidic chip for biological applications. The GaNAT demonstrated its ability to work on high power (up to 10W) with minimal cooling requirement while maintaining the device temperature below 32°C. Acoustofluidic modelling was successfully applied to numerically study and predict acoustic pressure field and particle trajectories within the GaNAT, which agree well with the experimental results on patterning polystyrene microspheres and two types of biological cells including fibroblast and renal tumour cells. The GaNAT allowed both cell types to maintain high viabilities of 84.5% and 92.1%, respectively.**

***Index Terms*— gallium nitride, surface acoustic wave, acoustic tweezer, cell manipulation**

I. Introduction

GaN is a compound semiconductor that has resulted in the revolution in performance and efficiency of light-emitting diode (LED) and power transistors [1]. GaN has tremendous potentials to facilitate new functionality over and beyond the silicon-based semiconductor industry which is currently faced with diminishing returns of performance versus cost. The distinct properties of GaN, i.e. its wide band gap, high breakdown electric field, and high electron mobility, make it an excellent candidate for the next generation power electronics [2, 3], high frequency communications [4], and photonic applications [5]. GaN is also known as a robust piezoelectric material for fabricating acoustic resonators and diverse electromechanical devices which are required to operate in harsh environments. Its biocompatibility and stability in aqueous environments have previously been demonstrated [6]. Recently, it is reported that GaN exhibits great potentials in biosensing [7], interacting with cells [8], and integrating with optoelectronics and transistors for sensor applications [9].

Acoustic tweezers are a versatile tool that can manipulate particles with sizes between nanometres and centimetres using acoustic waves with frequencies ranged from 1 kHz to 500 MHz [10]. Acoustic tweezers based on surface acoustic wave (SAW) devices have been developed to actuate nano- and micro-particles in the fields of two-dimensional [11] and three-

Manuscript received January, 1st, 2020. This work was supported in part by the Natural Science Foundation of China (81501472, 61704017), Engineering and Physical Sciences Research Council (EPSRC) fellowship EP/N01202X/2, EP/P002803/1 and EP/P018998/1, Global Challenges Research Fund (GCRF), and the Royal Society (IEC/NSFC/170142, IE161019).

F.W., D.J.W., J.W., H.W., R.T., R.M., X.Y. are with the Department of Electrical and Electronic Engineering, School of Engineering, Cardiff University, UK CF24 3AA, (corresponding author to provide phone: +44 (0) 2920875708; e-mail: yangx26@cf.ac.uk).

C.S., is with School of Life Sciences, Northwestern Polytechnical University, 710072, P.R. China (e-mail: chaosun@nwpu.edu.cn)

M.H.S., J.Y., are with the Preclinical Studies of Renal Tumours Group, Division of Cancer and Genetics, School of Medicine, Cardiff University, UK CF14 4XN (e-mail: ShenMH@cardiff.ac.uk, YangJ13@cardiff.ac.uk)

F.Y., is with the Department of Biomedical Engineering, School of Engineering, Duke University, NC 27708-0281, USA (e-mail: fyuan@duke.edu)

Z.X., is with the Department of Civil Engineering, School of Engineering, Cardiff University, UK CF24 (e-mail: ZXie@cardiff.ac.uk)

D.L., is with the Department of Engineering, University of Cambridge, UK CB2 1PZ (e-mail: dl359@cam.ac.uk)

C.A., is with the Tissue Microenvironment Group, Division of Cancer & Genetics, School of Medicine, Cardiff University, Cardiff, UK CF14 4XN (e-mail: ClaytonA@cardiff.ac.uk)

Y.Z., is with the Systems Immunity University Research Institute and Division of Infection and Immunity, School of Medicine, Cardiff University, Cardiff, UK CF14 4XN (e-mail: ZhouY58@cardiff.ac.uk)

Z.W., is with the School of Optoelectronic Engineering and Instrumentation Science, Dalian University of Technology, 116023, P.R. China (e-mail: zhenlinwu@dlut.edu.cn)

Y.F., is with the Faculty of Engineering and Environment, Northumbria University, Newcastle Upon Tyne, UK NE1 8ST (e-mail: richard.fu@northumbria.ac.uk)

W.X., is with the Department of Mechanical Engineering, Northwestern Polytechnical University, 710072, P.R. China (e-mail: xunwp@mail.nwpu.edu.cn)

dimensional cell manipulation [12], objects on water [13], protein crystallisation [14], reconfigurable manipulation of particles and cells [15], separation of circulating tumour cells [16] and extracellular vesicles [17-19], manipulation of nanoparticles [20], nanoscale confined fluids and particles [21] and droplets [22]. Acoustic tweezers have been integrated with dielectrophoresis [10] and optics [11] to perform delicate non-contact manipulation of various samples. The integration between acoustic tweezers and other techniques allows the development of miniaturized multiphysical platforms for maximizing the analysis to the sample [23].

A common piezoelectric material used for fabricating acoustic tweezers based on SAW is lithium niobate ($LiNbO_3$). However, bulk $LiNbO_3$-based SAW devices are generally brittle so that great care of handling and cooling is required to prevent thermal stress breakage of the $LiNbO_3$ [18, 19] when the device is operated at high input voltage/power. This limits the stability and performance of using these devices in high-throughput applications. Many III-V compound semiconductors including GaN, ZnO, and AlN show desired characteristics for SAW-based applications such as high temperature stability, low propagation loss, high SAW velocity, smooth surface, and high thermal conductivity [24]. ZnO provides slightly higher electromechanical coupling coefficient but has a low wave propagation velocity and shows high leakage thus limiting its uses at very high frequency. Also, its chemical stability and corrosion resistance are potential issues. Additionally, zinc is a dopant of silicon and its monolithic integration with silicon complementary metal-oxide-semiconductor (CMOS) circuits is challenging [25]. GaN can be manufactured as thin-film piezoelectric material since the acoustic velocity in GaN is very close to silicon which could result in low acoustic loss/mismatch [26]. In addition, the high performance that can be achieved in GaN electronic and optical devices offers a multitude of integration opportunities such as monolithic integration with control electronics based on GaN power amplifiers and optoelectronic devices to realise functionally diverse modules and versatile labs on a chip. Table 1 compares the key properties between GaN and $LiNbO_3$, which shows that GaN has a smaller effective coupling factor but much higher thermal conductivity.

Table 1-The comparison of properties between GaN and $LiNbO_3$

	Thermal Conductivity (W/(cm·K))	Elastic Modulus (GPa)	$k_{eff}^2(\%)$
GaN	1.3 [27]	60 [26]	2 [28]
$LiNbO_3$	0.044 [29]	398 [30]	5-12 [24]

In addition, it has also been demonstrated that two-dimensional electron gases (2DEG) on which GaN high electron mobility transistors (HEMTs) are based, can be used as interdigital transducers (IDTs) in SAW devices thus eliminating the mass loading and signal reflection caused by metal IDTs [31]. Such properties along with the maturity of GaN device manufacturing on large wafer sizes makes GaN a perfect choice for fabricating acoustic devices to monolithically integrate with power amplifier made by HEMTs for high-frequency, high-power, and high-temperature operation, with significantly reduced size, weight, and costs [26]. Despite extensive research that has been devoted to GaN, only limited attention has been paid to the implementation of GaN into acoustofluidic devices.

In this study, we describe a novel GaN-based Acoustic Tweezer (GaNAT) for the manipulation of live biological cells and polystyrene microspheres. The GaNAT demonstrated the capability to operate at high power with minimal need of cooling to trap and manipulate micro-particles and biological cells, while keeping high cell viability. The integration of GaN with microfluidics and the potential of using GaN in new generation nano and microelectromechanical systems (N/MEMS) will allow hitherto unobtainable levels of integration and compatibility of GaN with the electro-acoustic, electronic systems, and semiconductor system in particular.

II. WORKING PRINCIPLE

A schematic illustration of the GaNAT is shown in Fig. 1a. Comb-like metallic electrodes were patterned onto the GaN thin film grown on a sapphire substrate to form the IDTs. A polydimethylsiloxane (PDMS) microchannel was then bonded between the two IDTs for accommodating fluid samples containing microparticles/cells. The GaNAT was driven by applying radio frequency (RF) signals to generate SAWs with amplitudes of pico- to nano-meters, which are propagating on the surface of the GaN layer. Fig. 1b shows the counter-propagating SAWs generated by the IDTs to create a standing-SAW (SSAW) on the GaN layer, which forms a series of pressure nodes (PNs) and pressure anti-nodes (ANs) along the pathway. SSAWs produce leaky acoustic waves inside the fluid within the microchannel. The acoustic waves induce pressure disturbances in the fluid, which generate an acoustic radiation force, $\boldsymbol{F}^{\mathrm{rad}}$, on microparticles. $\boldsymbol{F}^{\mathrm{rad}}$ can drive a microparticle to move towards either PNs or ANs according to the sign of the acoustic contrast factor of the microparticle [32]. In addition, microparticles simultaneously experience a Stokes drag force, $\boldsymbol{F}^{\mathrm{drag}}$, when they are moving in the fluid [33]. Buoyancy and gravitational forces are generally negligible. Polystyrene microspheres and biological cells typically possess a positive acoustic contrast factor which allows them to be attracted towards the nearest PN [34].

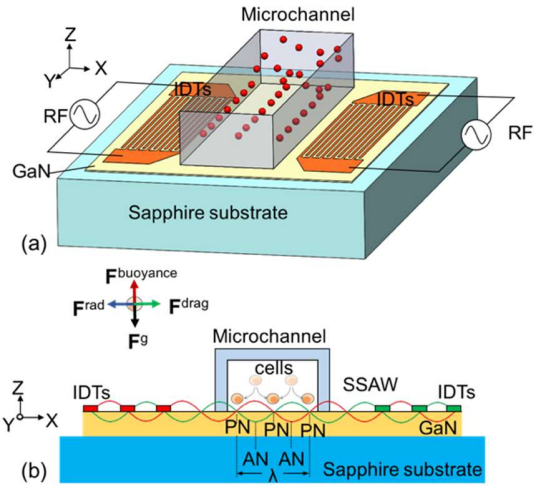

Fig. 1. (a) Schematic illustration of GaN-based Acoustic Tweezer (GaNAT). (b) Four types of forces applied on a particle inside the GaNAT, and the cell

patterning on pressure nodes (PN) driven by standing surface acoustic waves (SSAW) generated by GaN interdigital transducers (IDTs).

III. EXPERIMENTAL METHODS

A. Device fabrication and setup

The fabricated GaNAT device is shown in Fig. 2a. Comb-like metallic electrodes were patterned onto a ~ 4.5 μm thick undoped GaN thin film grown on [0001] direction of a ~ 600 μm thick sapphire substrate. This epitaxial orientation [0001] was used as this is the polar direction in GaN and therefore offers the strongest piezoelectric response. Patterning of the IDTs was done by using conventional photolithography. A positive photoresist (EPI680, Everlight Advanced Chemicals Ltd, Suzhou, China) was used for spinning on the substrate followed by mask alignment. The metal bilayers (Cr/Au, 30 nm/150 nm) were deposited onto the patterned wafer using a magnetron sputtering system (LLJGP-560, SKY technology development, Shen Yang, China). The chromium layer was used to provide adequate adhesion between the gold electrodes and the GaN thin film. The wafer was then placed into acetone to perform a lift-off process. Then, the wafer was cleaned with ethanol, deionized water and dried with nitrogen. The width and pitch of the finger electrodes are both 70 μm, which gives a SSAW wavelength of $\lambda = 280$ μm. The two IDTs' centre-to-centre spacing was 18 λ and each IDT consisted of 40 pairs of finger electrodes. A silicon mould for making the PDMS microchannel with the channel dimension of 1 cm (L) × 280 μm (W) × 60 μm (H) was manufactured using a standard soft-lithography process. The microchannel was made by a mixture of Sylgard 184 silicone elastomer base and curing agent (Dow Corning, MI) at a mass ratio of 10:1. The mixture was degassed and cast onto the silicon mould and then cured at 65ºC for 3 hours. The PDMS microchannel was mechanically bonded to the centre of the GaN SAW device (between the two IDTs) to construct the GaNAT (Fig. 2a). The GaNAT was mounted onto a heatsink (10 cm (L) × 10 cm (W) × 4 cm (H)) coupling by thermal grease. Inlet and outlet tubes were connected to the microchannel for flowing fluid samples.

The experimental configuration is shown in Fig. 2b. The RF signal produced by a signal generator was amplified by a power amplifier and then coupled onto the GaNAT. To enable the maximum RF power delivered from the power amplifier to the IDTs for actuating microparticles/cells, impedance L-matching networks were designed for both the IDTs. The forward and reflected powers of each IDT were monitored using two power meters (U2004A, Keysight Technologies, UK).

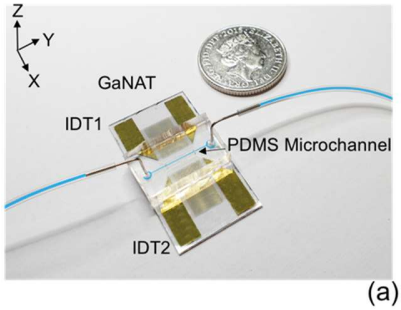

(a)

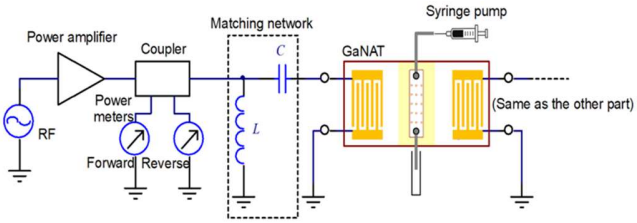

(b)

Fig. 2. GaN-based acoustic tweezer (GaNAT) and the experiment. (a) The photo of GaNAT consisted of the GaN IDTs bonded with the PDMS microchannel. (b) The test and experiment setup of the GaNAT.

B. Device characterization

To investigate how the bonded microchannel affects the transfer functions of the GaN SAW device, a vector network analyser (VNA, E5061B ENA, Keysight) was used to measure the transfer functions of the two IDTs, S_{11} (reflection coefficient) and S_{21} (transmission coefficient), with and without the microchannel in place. The IDT's surface temperature was seen to increase using an infrared thermal camera (ETS320, FLIR, US), with increasing input power. The measuring point was set on the metal electrodes which produced most joule heat to represent the highest temperature on the GaNAT. The spatial resolution of the thermal camera is 21 μm, which is approximately one third of the width of the finger electrodes. Due to the RF excitation that induces Joule effect on finger electrodes [35], the spatial resolution of the camera is able to accurately detect the temperature distribution on the IDTs after correcting for the emissivity of the material. The temperature was measured without microchannel and each measurement was taken once the temperature reading stabilised.

To investigate the SAW amplitude produced on the GaNAT and compare with that of a conventional $LiNbO_3$ SAW device, a SAW device made from $LiNbO_3$ with the similar frequency (20 MHz) was fabricated. A laser vibrometer (PSV-500-VH, Polytec, Germany) was used to quantify the SAW amplitudes on both devices under the same input power of 1 W.

C. Numerical simulation

A numerical model was applied to investigate the acoustofluidic conditions of the GaNAT and to predict the trajectory of microparticles [36, 37]. The model is valid for the GaNAT as the microchannel length is significantly longer than its height and width, and the acoustic waves are uniform along and perpendicular to the main flow direction. In this case, the acoustic pressure and microparticle movement can be investigated with a two-dimensional cross-sectional model. COMSOL Multiphysics® version 5.4 was used to solve the first-order acoustic pressure fields and microparticle trajectories.

D. Sample preparation

A microparticle sample was prepared using 10 μm polystyrene microspheres (Sigma Aldrich, Germany) mixed with phosphate-buffered saline (PBS) with a concentration of 2% (vol/vol) to verify the numerical results and the GaNAT performance. A syringe pump (WZ-74905, Cole-Parmer, US) was used to slowly introduce the polystyrene microspheres to

the microchannel until an evenly dispersed pattern was seen and became stable.

Biological cells were used to explore the potential of manipulation cells using the GaNAT and to test whether the GaNAT was able to maintain cell viability during acoustic actuation. Two types of biological cells, e.g., mouse renal tumour cells (TSC1-associated tumour cells, Tsc1-204) [38] and mouse fibroblast cells (MEF, Tsc1-387-2) [39], were prepared for the test. These two types of cells are widely used to investigate mechanisms of tuberous sclerosis-associated renal tumourigenesis and oncogenic pathway. They are quite different in their sizes, morphologies, and genotypes, and thus are easily recognized in the subsequent analysis. The sizes and viabilities of the cells were measured by a cell counter (NC-3000, Chemometec, Denmark). Mouse renal tumour cells and fibroblast cells were cultured using Dulbecco's Modified Eagle Medium (DMEM) (Gibco, Thermo Fisher, UK) containing 10% fetal bovine serum, 50 units/ml penicillin and 50 µg/ml streptomycin at 37ºC in a humidified incubator with 5% (vol/vol) CO_2 atmosphere. Before introducing to the device, the adherent cells were rendered into suspension by exposure to trypsin, followed by dilution into PBS at a concentration of 1×10^6 cells/ml. Cell samples were stored in Eppendorf tubes within an ice bath to keep the temperature at 4°C during the experiment. To assess cell viability, acridine orange (30 µg/ml) and diaminophenylindole (100 µg/ml) were used to stain the sample at a ratio of 1:20. The stained sample was pipetted onto a counter slide and analysed by the cell counter. For the viability study, both the fibroblast and renal tumour cells were divided into two groups: SSAW ON group - cells passing through the GaNAT with SSAW present, and SSAW OFF group - those without SSAW present. To mimic the flow condition for cell separation, the flow rate of the two groups going through the GaNAT was set to 20 µL/min [16].

When the microparticles or cells were introduced to the microchannel, RF signals were applied to the two IDTs to generate SSAWs in the microchannel. The two phase differences (0º and 180º) of the two RF signal was investigated against the pattern of the microparticles or cell aggregation.

IV. Results and Discussion

A. Characterization of the GaNAT

The results of S_{11} and S_{21} spectra of the SAW devices without microchannel (solid lines) and with microchannel (dotted lines) are shown in Figs. 3a and 3b, respectively, where the lower frequency peaks at 19.40 MHz corresponds to the Rayleigh mode and 38.91 MHz corresponds to the Sezawa mode.

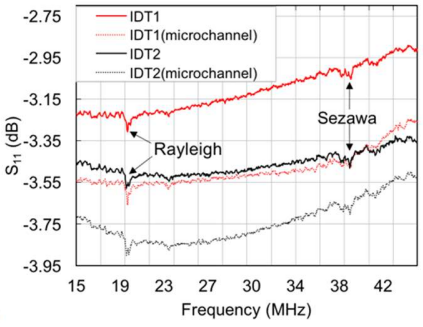

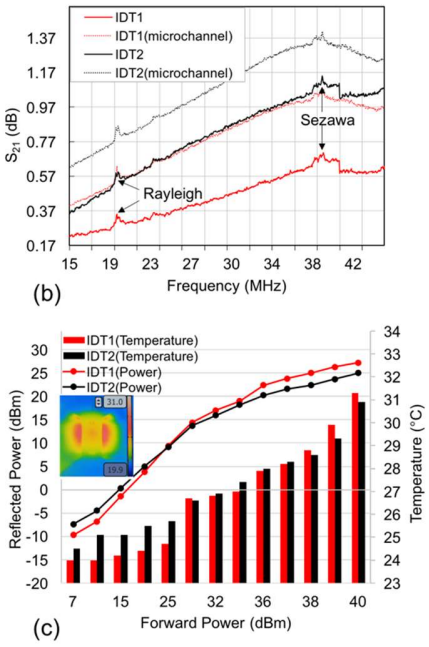

Fig. 3. The characterization of GaN IDTs. (a) The S11 parameter of the two IDTs with and without the presence of the microchannel. (b) The S21 parameter of the two IDTs with and without the presence of the microchannel. Red and black curves are the parameter for IDT1 and IDT2, respectively. Solid and dotted curves represent the measurement without and with the microchannel. Both the Rayleigh and Sezawa mode frequencies are noted on the curves. (c) Measurement of the temperature of the IDTs and the reflected power while increasing the forward power, inset is the thermal image of the GaN IDTs.

Due to the small dispersion value ($k\mathrm{h_{GaN}} = 2\pi\mathrm{h_{GaN}}/\lambda \approx 0.1$, where k is the wave number, $\mathrm{h_{GaN}}$ is the thickness of GaN layer), the SAW velocity approximates the acoustic velocity in sapphire, i.e. $v_{\mathrm{Ray}}^{\mathrm{sapp}}$=5,486 m/s in the $[1\bar{1}00]$ direction [40], which gives the calculated Rayleigh frequency as $f = v_{\mathrm{Ray}}^{\mathrm{sapp}}/\lambda \approx 19.59$ MHz. The slight difference between the measured and calculated frequencies may be due to the mismatching between the GaN and sapphire layers. The Rayleigh frequency of 19.40 MHz was used in the following experiments. In general, both the S_{11} and S_{21} parameters show that adding PDMS microchannel does not deteriorate the frequency characteristics of the GaNAT. The relatively small peaks in S_{11} and S_{21} spectra are mainly due to the low thickness of the GaN film. The electromechanical coupling coefficient, k^2, was estimated to be 0.04±0.005% ($h/\lambda = 0.016$, h is the layer thickness, λ is the SAW wavelength) according to the method introduced by [41, 42].

The temperature rise on the IDTs as the consequence of the increased forward power, and the relationship between forward powers and reverse powers on the IDTs are plotted in Fig. 3c. The inset was the thermal image of the IDTs at 10 W. At a room temperature of 24°C, the temperature on the IDTs was increased to ~31°C at 10 W, which was the maximum power supplied to the GaNAT in this study. Without using any active cooling system such as Peltier cooler [18], the GaNAT was able to effectively convert RF powers to SAWs while keeping the device temperature below the biological limit.

Under an input power of 1 W, the SAW vibration amplitudes at the centre between the two IDTs on the GaNAT and $LiNbO_3$ devices were found to be 123.2±2.4 pm (average ± SD) and

1,650.8±16.4 pm (average ± SD), respectively. The smaller vibration amplitude produced by GaN is due to its lower k^2, which implies that the device would have difficulty in agitating liquid, or transport droplets, but the data shown here clearly demonstrates that it is sufficient to generate the SSAW for manipulation of particles and cells. However, we could improve the k^2 by increasing the GaN film thickness, film quality, or using doped-GaN epilayer [41]. The minimum input powers to fully trap 10-μm polystyrene microspheres to the PNs inside the GaNAT and $LiNbO_3$ devices are ~1.9 W and ~0.2 W, respectively.

B. Numerical simulation and manipulation of microspheres

The simulation results of the acoustic pressure and the microparticle trajectories are shown in Figs. 4a –d. Fig. 4a demonstrates the first-order acoustic pressure field with no phase difference ($\Delta\varphi$=0°) between the RF signals driving the two IDTs, which results in the PNs located at the middle and two sides of the microchannel. Fig. 4c shows the corresponding microparticle trajectories which produce three microparticle traces on the PNs. The width of the microchannel in this study is the same as the SSAW's wavelength ($\lambda = 280$ μm) allowing the microparticles to aggregate at three positions inside the microchannel. The PN distribution can be achieved by setting the phase difference of the two IDTs to $\Delta\varphi$ =0°. By adding the phase difference to $\Delta\varphi$ =180°, one can position the ANs to be at the middle and two sides of the microchannel (Fig. 4b), which leads to five microparticle traces as shown in Fig. 4d. Polystyrene microspheres were then introduced to the GaNAT to test the simulation results. When they were evenly dispersed inside the microchannel, the RF signals with $\Delta\varphi$=0° were applied to the GaNAT and then 10 μm polystyrene microspheres were immediately shifted to the three PN traces as the microscopic top-view image shown in Fig. 4e. When the RF signals with $\Delta\varphi$=180° were applied, five microsphere traces were generated inside the microchannel as shown in Fig. 4f. The good agreement between the numerical prediction and experimental observation demonstrated the ability of GaNAT in actuating and trapping microspheres in a controllable pattern.

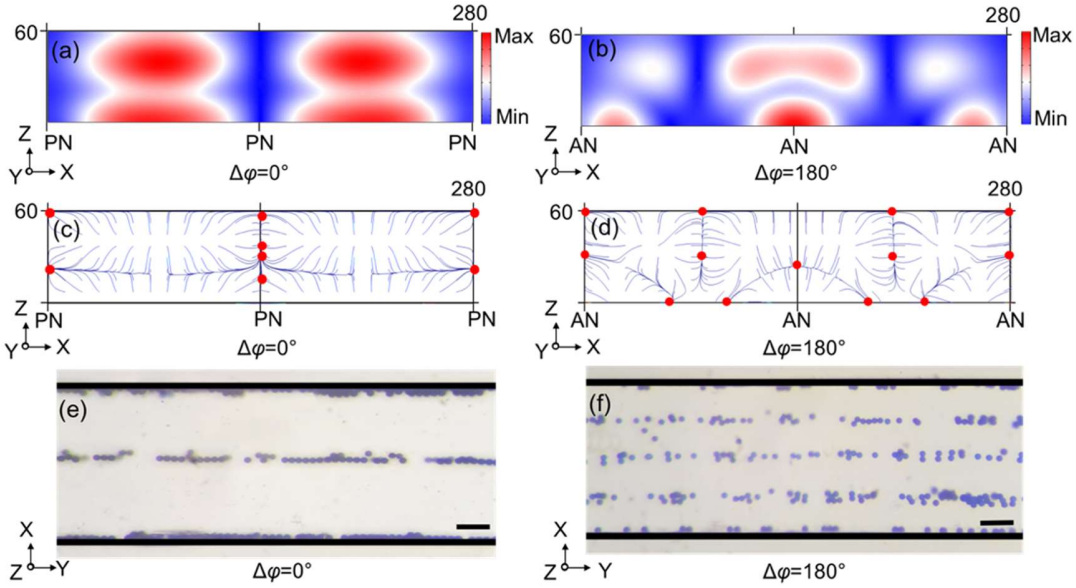

Fig. 4. Numerical and experimental studies of the GaNAT. (a) and (b): acoustic pressure field inside the microchannel for the pressure node (PN) and pressure anti-node (AN) located at the middle of the channel, respectively. (c) and (d): particle trajectories of 10 μm polystyrene microspheres actuated by the corresponding acoustic pressures in (a) and (b). (e) and (f): microscope images of the polystyrene microsphere patterned in the GaNAT. The scale bar is 50 μm.

C. Manipulation of cells

After the microsphere verification, cells were introduced to the GaNAT. When the PNs were set at the middle and two sides of the microchannel ($\Delta\varphi$=0°), the cells were aggregated at three traces with the majority trapped in the centre of the microchannel (Fig. 5a). By switching to 180° phase difference ($\Delta\varphi$=180°), the three traces immediately changed into five as shown in Fig. 5b. The cell trapping patterns agreed well with the numerical predication and the microsphere results.

The cell viabilities of the SSAW ON and OFF groups with the comparison with original samples (control group) were tested and shown in Fig. 5c. For the SSAW ON group, the viabilities of the renal tumour cells and fibroblast cells were 84.5% and 92.1%, respectively. For the SSAW OFF group, the viabilities were 88.1% and 96.9%, respectively. For these two groups, fibroblast cells showed higher viabilities because they are more tolerable to the changes in temperature and/or CO_2 concentration after they were removed from the incubator. Both the cell types denoted slightly lower viabilities in the SSAW-ON Group, which is mainly attributed to the heat produced on-chip at high input powers. Nevertheless, both the cell types showed good cell viability after acoustic manipulation using the GaNAT.

V. Conclusion

Despite the electromechanical coupling coefficient of GaN being lower than $LiNbO_3$, the use of GaN to develop acoustic tweezer made by GaN-based IDTs working at megahertz frequencies for manipulating cells and microparticles has been demonstrated. As a novel thin-film piezoelectric material for fabricating acoustofluidic devices, GaN/sapphire structure can be used to generate Rayleigh and Sezawa waves. The GaNAT denoted an excellent thermal stability when operated at high

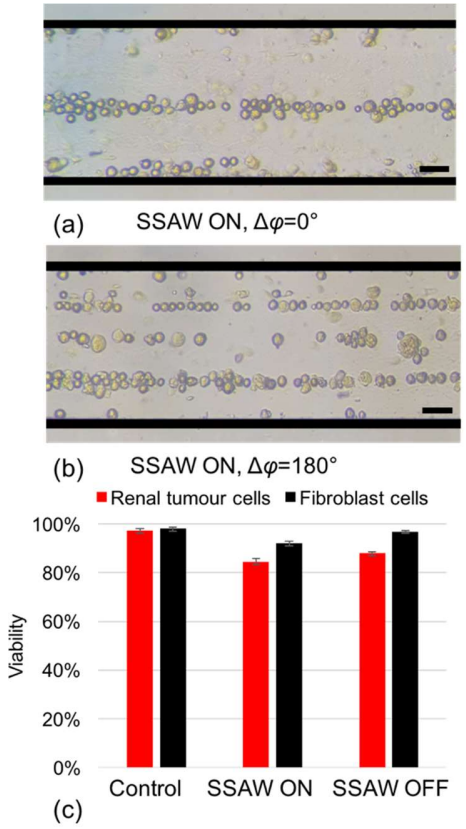

Fig. 5. Cell manipulation and viability test. (a) and (b) are the cells patterning in the GaNAT for the pressure node and pressure anti-node located at the middle of the channel, respectively. (c) shows the viabilities of the control, SAW ON and SAW OFF groups. The scale bar is 50 μm.

input power. The thermal performance could be further improved by using Si as a substrate and this would also offer compatibility with high yield, high volume low cost semiconductor manufacturing to significantly reduce the cost of these devices. The numerical simulation results for the GaNAT were validated using the experimental results of microparticles and cell manipulation. Acoustophoresis realised by the GaNAT will open the area of exploring multiphysical application of GaN towards monolithic integration with electronics for developing biosensors and N/MENS.

REFERENCES

[1] H. Amano, Y. Baines, E. Beam, M. Borga, T. Bouchet, P. R. Chalker, M. Charles, K. J. Chen, N. Chowdhury, R. Chu, C. De Santi, M. M. De Souza, S. Decoutere, L. Di Cioccio, B. Eckardt, T. Egawa, P. Fay, J. J. Freedsman, L. Guido, O. Häberlen, G. Haynes, T. Heckel, D. Hemakumara, P. Houston, J. Hu, M. Hua, Q. Huang, A. Huang, S. Jiang, H. Kawai, D. Kinzer, M. Kuball, A. Kumar, K. B. Lee, X. Li, D. Marcon, M. März, R. McCarthy, G. Meneghesso, M. Meneghini, E. Morvan, A. Nakajima, E. M. S. Narayanan, S. Oliver, T. Palacios, D. Piedra, M. Plissonnier, R. Reddy, M. Sun, I. Thayne, A. Torres, N. Trivellin, V. Unni, M. J. Uren, M. Van Hove, D. J. Wallis, J. Wang, J. Xie, S. Yagi, S. Yang, C. Youtsey, R. Yu, E. Zanoni, S. Zeltner, and Y. Zhang, "The 2018 GaN power electronics roadmap," *Journal of Physics D: Applied Physics,* vol. 51, no. 16, p. 163001, 2018.10.1088/1361-6463/aaaf9d

[2] J. Kuzmik, "Power electronics on InAlN/(In)GaN: Prospect for a record performance," *IEEE Electron Device Letters,* vol. 22, no. 11, pp. 510-512, 2001.10.1109/55.962646

[3] B. J. Baliga, "Gallium nitride devices for power electronic applications," *Semiconductor Science and Technology,* vol. 28, no. 7, p. 074011, 2013.10.1088/0268-1242/28/7/074011

[4] A. M. Eblabla, X. Li, D. J. Wallis, I. Guiney, and K. Elgaid, "GaN on Low-Resistivity Silicon THz High-Q Passive Device Technology," *IEEE Transactions on Terahertz Science and Technology,* vol. 7, no. 1, pp. 93-97, 2017.10.1109/TTHZ.2016.2618751

[5] S. Kako, C. Santori, K. Hoshino, S. Götzinger, Y. Yamamoto, and Y. Arakawa, "A gallium nitride single-photon source operating at 200 K," *Nature Materials,* vol. 5, no. 11, pp. 887-892, 2006.10.1038/nmat1763

[6] S. A. Jewett, M. S. Makowski, B. Andrews, M. J. Manfra, and A. Ivanisevic, "Gallium nitride is biocompatible and non-toxic before and after functionalization with peptides," *Acta Biomaterialia,* vol. 8, no. 2, pp. 728-733, 2012/02/01/ 2012.10.1016/j.actbio.2011.09.038

[7] R. Kirste, N. Rohrbaugh, I. Bryan, Z. Bryan, R. Collazo, and A. Ivanisevic, "Electronic Biosensors Based on III-Nitride Semiconductors," *Annual Review of Analytical Chemistry,* vol. 8, no. 1, pp. 149-169, 2015.10.1146/annurev-anchem-071114-040247

[8] P. J. Snyder, D. R. LaJeunesse, P. Reddy, R. Kirste, R. Collazo, and A. Ivanisevic, "Bioelectronics communication: encoding yeast regulatory responses using nanostructured gallium nitride thin films," *Nanoscale,* 10.1039/C8NR03684E vol. 10, no. 24, pp. 11506-11516, 2018.10.1039/C8NR03684E

[9] F. Calle, J. Pedrós, T. Palacios, and J. Grajal, "Nitride-based surface acoustic wave devices and applications," *Physica Status Solidi,* vol. 2, no. 3, pp. 976-983, 2005.10.1002/pssc.200460605

[10] A. Ozcelik, J. Rufo, F. Guo, Y. Gu, P. Li, J. Lata, and T. J. Huang, "Acoustic tweezers for the life sciences," *Nature Methods,* Review vol. 15, no. 12, pp. 1021-1028, 2018.10.1038/s41592-018-0222-9

[11] D. J. Collins, B. Morahan, J. Garcia-Bustos, C. Doerig, M. Plebanski, and A. Neild, "Two-dimensional single-cell patterning with one cell per well driven by surface acoustic waves," *Nature Communications,* Article vol. 6, p. 8686, 2015.10.1038/ncomms9686

[12] F. Guo, Z. Mao, Y. Chen, Z. Xie, J. P. Lata, P. Li, L. Ren, J. Liu, J. Yang, M. Dao, S. Suresh, and T. J. Huang, "Three-dimensional manipulation of single cells using surface acoustic waves," *Proceedings of the National Academy of Sciences of the United States of America,* Article vol. 113, no. 6, pp. 1522-1527, 2016.10.1073/pnas.1524813113

[13] P. Zhang, C. Chen, F. Guo, J. Philippe, Y. Gu, Z. Tian, H. Bachman, L. Ren, S. Yang, Z. Zhong, P.-H. Huang, N. Katsanis, K. Chakrabarty, and T. J. Huang, "Contactless, programmable acoustofluidic manipulation of objects on water," *Lab on a Chip,* 10.1039/C9LC00465C vol. 19, no. 20, pp. 3397-3404, 2019.10.1039/C9LC00465C

[14] Y. Zhang, C. Devendran, C. Lupton, A. de Marco, and A. Neild, "Versatile platform for performing protocols on a chip utilizing surface acoustic wave (SAW) driven mixing," *Lab on a Chip,* 10.1039/C8LC01117F vol. 19, no. 2, pp. 262-271, 2019.10.1039/C8LC01117F

[15] Z. Tian, S. Yang, P. H. Huang, Z. Wang, P. Zhang, Y. Gu, H. Bachman, C. Chen, M. Wu, Y. Xie, and T. J. Huang, "Wave number–spiral acoustic tweezers for dynamic and reconfigurable manipulation of particles and cells," *Science Advances,* Article vol. 5, no. 5, 2019.10.1126/sciadv.aau6062

[16] P. Li, Z. Mao, Z. Peng, L. Zhou, Y. Chen, P. H. Huang, C. I. Truica, J. J. Drabick, W. S. El-Deiry, M. Dao, S. Suresh, and T. J. Huang, "Acoustic separation of circulating tumor cells," *Proceedings of the National Academy of Sciences of the United States of America,* Article vol. 112, no. 16, pp. 4970-4975, 2015.10.1073/pnas.1504484112

[17] K. Lee, H. Shao, R. Weissleder, and H. Lee, "Acoustic Purification of Extracellular Microvesicles," *ACS Nano,* vol. 9, no. 3, pp. 2321-2327, 2015.10.1021/nn506538f

[18] M. Wu, Y. Ouyang, Z. Wang, R. Zhang, P. H. Huang, C. Chen, H. Li, P. Li, D. Quinn, M. Dao, S. Suresh, Y. Sadovsky, and T. J. Huang, "Isolation of exosomes from whole blood by integrating acoustics and microfluidics," *Proceedings of the National Academy of Sciences of the United States of America,* Article vol. 114, no. 40, pp. 10584-10589, 2017.10.1073/pnas.1709210114

[19] M. Wu, C. Chen, Z. Wang, H. Bachman, Y. Ouyang, P.-H. Huang, Y. Sadovsky, and T. J. Huang, "Separating extracellular vesicles and lipoproteins via acoustofluidics," *Lab on a Chip,* 10.1039/C8LC01134F vol. 19, no. 7, pp. 1174-1182, 2019.10.1039/C8LC01134F

[20] D. J. Collins, Z. Ma, J. Han, and Y. Ai, "Continuous micro-vortex-based nanoparticle manipulation via focused surface acoustic waves," *Lab on a Chip,* Article vol. 17, no. 1, pp. 91-103, 2017.10.1039/C6LC01142J

[21] M. Miansari and J. R. Friend, "Acoustic Nanofluidics via Room-Temperature Lithium Niobate Bonding: A Platform for Actuation and Manipulation of Nanoconfined Fluids and Particles," vol. 26, no. 43, pp. 7861-7872, 2016.10.1002/adfm.201602425

[22] R. J. Shilton, M. Travagliati, F. Beltram, and M. Cecchini, "Nanoliter-droplet acoustic streaming via ultra high frequency surface acoustic waves," *Advanced Materials,* vol. 26, no. 29, pp. 4941-4946, 2014.10.1002/adma.201400091

[23] S. Haeberle and R. Zengerle, "Microfluidic platforms for lab-on-a-chip applications," *Lab on a Chip,* 10.1039/B706364B vol. 7, no. 9, pp. 1094-1110, 2007.10.1039/B706364B

[24] Y. Q. Fu, J. K. Luo, N. T. Nguyen, A. J. Walton, A. J. Flewitt, X. T. Zu, Y. Li, G. McHale, A. Matthews, E. Iborra, H. Du, and W. I. Milne, "Advances in piezoelectric thin films for acoustic biosensors, acoustofluidics and lab-on-chip applications," *Progress in Materials Science,* Review vol. 89, pp. 31-91, 2017.10.1016/j.pmatsci.2017.04.006

[25] H. Bhugra and G. Piazza, *Piezoelectric MEMS Resonators*. Spinger, 2017. 10.1007/978-3-319-28688-4

[26] M. Rais-Zadeh, V. J. Gokhale, A. Ansari, M. Faucher, D. Théron, Y. Cordier, and L. Buchaillot, "Gallium Nitride as an Electromechanical Material," *Journal of Microelectromechanical Systems,* vol. 23, no. 6, pp. 1252-1271, 2014.10.1109/JMEMS.2014.2352617

[27] M. D. Kamatagi, N. S. Sankeshwar, and B. G. Mulimani, "Thermal conductivity of GaN," *Diamond and Related Materials,* vol. 16, no. 1, pp. 98-106, 2007.10.1016/j.diamond.2006.04.004

[28] V. Gokhale, Y. Shim, and M. Rais-Zadeh, *Observation of the Acoustoelectric Effect in Gallium Nitride Micromechanical Bulk Acoustic Filters*. 2010, pp. 524-529. 10.1109/FREQ.2010.5556273

[29] S. Yao, J. Wang, H. Liu, X. Hu, H. Zhang, X. Cheng, and Z. Ling, "Growth, optical and thermal properties of near-stoichiometric LiNbO3 single crystal," *Journal of Alloys and Compounds,* vol. 455, no. 1, pp. 501-505, 2008.10.1016/j.jallcom.2007.02.001

[30] H. Ledbetter, H. Ogi, and N. Nakamura, "Elastic, anelastic, piezoelectric coefficients of monocrystal lithium niobate," *Mechanics of Materials,* vol. 36, no. 10, pp. 941-947, 2004.10.1016/j.mechmat.2003.08.013

[31] K. Wong, W. Tang, K. M. Lau, and K. J. Chen, "Planar Two-dimensional Electron Gas (2DEG) IDT SAW Filter on AlGaN/GaN Heterostructure," *2007 IEEE/MTT-S International Microwave Symposium,* pp. 2043-2046, 2007.10.1109/MWSYM.2007.380252

[32] M. Settnes and H. Bruus, "Forces acting on a small particle in an acoustical field in a viscous fluid," *Physical Review E - Statistical, Nonlinear, and Soft Matter Physics,* Article vol. 85, no. 1, 2012, Art. no. 016327.10.1103/PhysRevE.85.016327

[33] N. Nama, R. Barnkob, Z. Mao, C. J. Kähler, F. Costanzo, and T. J. Huang, "Numerical study of acoustophoretic motion of particles in a PDMS microchannel driven by surface acoustic waves," *Lab on a Chip,* Article vol. 15, no. 12, pp. 2700-2709, 2015.10.1039/c5lc00231a

[34] M. A. Faridi, H. Ramachandraiah, I. Iranmanesh, D. Grishenkov, M. Wiklund, and A. J. B. M. Russom, "MicroBubble activated acoustic cell sorting," *Biomedical Microdevices,* vol. 19, no. 2, p. 23, 2017. 10.1007/s10544-017-0157-4

[35] L. Thevenard, I. Camara, J. Y. Prieur, P. Rovillain, A. Lemaitre, C. Gourdon, and J. Y. Duquesne, "Strong reduction of the coercivity by a surface acoustic wave in an out-of-plane magnetized epilayer," *Physical Review B,* vol. 93, 2016.10.1103/PhysRevB.93.140405

[36] Z. Mao, Y. Xie, F. Guo, L. Ren, P. H. Huang, Y. Chen, J. Rufo, F. Costanzo, and T. J. Huang, "Experimental and numerical studies on standing surface acoustic wave microfluidics," *Lab on a Chip,* Article vol. 16, no. 3, pp. 515-524, 2016.10.1039/c5lc00707k

[37] P. B. Muller, R. Barnkob, M. J. H. Jensen, and H. Bruus, "A numerical study of microparticle acoustophoresis driven by acoustic radiation forces and streaming-induced drag forces," *Lab on a Chip,* Article vol. 12, no. 22, pp. 4617-4627, 2012.10.1039/c2lc40612h

[38] J. Yang, M. Kalogerou, J. Gallacher, J. R. Sampson, and M. H. Shen, "Renal tumours in a Tsc1+/- mouse model show epigenetic suppression of organic cation transporters Slc22a1, Slc22a2 and Slc22a3, and do not respond to metformin," (in eng), *European journal of cancer,* vol. 49, no. 6, pp. 1479-90, 2013.10.1016/j.ejca.2012.10.027

[39] J. Yang, M. Kalogerou, P. A. Samsel, Y. Zhang, D. F. R. Griffiths, J. Gallacher, J. R. Sampson, and M. H. Shen, "Renal tumours in a Tsc2(+/-) mouse model do not show feedback inhibition of Akt and are effectively prevented by rapamycin," *Oncogene,* vol. 34, no. 7, pp. 922-31, 2015. 10.1016/j.ejca.2012.10.027

[40] J. Pedrós, F. Calle, J. Grajal, R. J. Jiménez Riobóo, C. Prieto, J. L. Pau, J. Pereiro, M. Hermann, M. Eickhoff, and Z. Bougrioua, "Anisotropic propagation of surface acoustic waves on nitride layers," *Superlattices and Microstructures,* vol. 36, no. 4, pp. 815-823, 2004.10.1016/j.spmi.2004.09.044

[41] X. Xu and R. C. Woods, "On the piezoelectric coupling constant of epitaxial Mg-doped GaN," *Solid-state Electronics - SOLID STATE ELECTRON,* vol. 54, pp. 680-684, 07/01 2010.10.1016/j.sse.2010.03.011

[42] R. C. Woods and F. A. Boroumand, "Comments on "Epitaxially grown GaN thin-film SAW filter with high velocity and low insertion loss"," *Ieee Transactions on Electron Devices,* vol. 53, no. 1, pp. 173-176, 2006.10.1109/ted.2005.860657